The effect of temperature on adhesion forces between surfaces and model foods containing whey protein and sugar

Journal Item

THE EFFECT OF TEMPERATURE ON ADHESION FORCES BETWEEN SURFACES AND MODEL FOODS CONTAINING WHEY PROTEIN AND SUGAR

KR Goode[1], J Bowen[1], N Akhtar[2], PT Robbins[1], PJ Fryer[1*].

[1]School of Chemical Engineering, University of Birmingham, Edgbaston, Birmingham, B15 2TT, UK.

[2]Eon UK, Westwood Business Park, Coventry CV4 8LG.

* Corresponding author email: p.j.fryer@bham.ac.uk

* Corresponding author telephone: +44 (0) 121 414 5451

ABSTRACT

The formation of fouling deposit from foods and food components is a severe problem in food processing and leads to frequent cleaning. The design of surfaces that resist fouling may decrease the need for cleaning and thus increase efficiency. Atomic force microscopy has been used to measure adhesion forces between stainless steel (SS) and fluoro-coated glass (FCG) microparticles and the model food deposits (i) whey protein (WPC), (ii) sweetened condensed milk, and (iii) caramel. Measurements were performed over a range of processing temperatures between 30-90ºC and at contact times up to 60 s. There is a significant increase in adhesion force of both types of microparticle to WPC at 90°C for all contact times. For confectionary deposits adhesion to SS was similar. Adhesion of confectionary deposits to FCG at 30°C revealed a decrease in adhesion compared to SS; at higher temperatures the adhesion forces were similar.

1. INTRODUCTION

1.1 FOULING AND CLEANING

During food processing thermally labile components build up on heat transfer surfaces resulting in fouling deposits. If these deposits are not removed regularly, production limiting effects typically occur (Fryer et al., 2006) such as

- Decreased heat transfer and product flow,
- Deviations in product consistency and quality,
- Increased risk to product safety.

Fouling is a costly problem in the food and beverage industry which is difficult to avoid. The reactions that lead to fouling result from the heat treatments needed to give pasteurisation or sterilisation and thus to ensure food safety. Fouling results from the adhesion of components of the fluid at the elevated temperatures employed in processing. To combat fouling and risk to food safety and quality, rigorous and frequent cleaning is employed. In food processing applications CIP (Cleaning-in-Place) systems are typically used to return the surface to a clean state (Tamine, 2008). Although these systems are effective, it is often unclear if they are optimal and new methods for characterising and measuring cleaning efficiency are needed. (Fryer and Asteriadou, 2009).

Most of the literature on food fouling has studied microorganisms or milk components (such as whey protein, which contains the protein β-lactoglobulin (β-lg) that forms the majority of milk pasteuriser deposit (Changani et al., 1997), but a wide range of deposits are formed depending on the chemistry of the material being processed. There is a need to understand the fouling and cleaning of a range of foodstuffs and their sensitivity to process variables such as temperature and shear stress (Christian and Fryer, 2006).

1.2 AFM IN FOULING AND CLEANING

Atomic force microscopy (AFM) is a sophisticated tool to study deposit-surface interactions at the nanoscale (Binnig et al., 1986). A cantilever (or probe) contacts the surface or deposit and the force of detachment can be determined from force-distance data. For reviews, see Morris (2004), and Liu and Wang (2011). Verran et al., (2000) studied stainless steel (SS) food contact surfaces by AFM and produced surfaces covering a range of R_a (roughness) values and topographies which were compared to new test surfaces. Using AFM, the authors found similar R_a values for new and worn surfaces although the topography was clearly different. Akhtar (2010) characterized the average roughness of four materials: 316L SS, ceramic, glass and poly(tetrafluoroethylene)-analogue; all were found to exhibit R_a < 0.8 µm.

1.2.1 MICROBIAL ADHESION

Verran et al., (2000) found the pattern of attachment of biofouling to new and worn surfaces was different (although the number of microbes attached was similar) which may affect surface cleanability. Whitehead et al., (2006) used AFM to assess the ease of removing *P. aeruginosa* (rods 1 µm width by 3 µm length) and *S. aureus* (1 µm sphere) from a titanium dioxide surface that was smooth or with defined surface features of 0.5 µm. To determine the ease of bacterial removal, scans were carried out with increasing force perpendicular to the cantilever tip. *S. aureus* cells were removed more easily from smooth surfaces, whereas *P. aeruginosa* cells were removed more easily from the surfaces with the defects. These findings suggest that cell shape/orientation and surface topography, and therefore

contact area, are important parameters in determining the maximum force required for bacterial detachment from surfaces.

Bowen et al., (2000) used AFM to characterise the adhesion of a fungal spore to mica at different pH: 3, 5, 7 and 9 (at 10^{-2} M). An increase in pH decreased the adhesion force from around 15 - 19 nN (at pH 3 and 5) to 3.5 nN (at pH 7 and 9). Sheng et al., (2008) used AFM to investigate the adhesion of *Pseudomonas* and sulphate-reducing bacteria to SS at different pH: 3, 5, 7 and 9. For *Pseudomonas*, at low and high pH (3 and 9) the adhesion force was greatest at around 2.5 nN. For *D. desulfricans* an increase in pH tended to decrease the adhesion force from 2.5 to 0.5 nN. Metal surfaces become negatively charged when the pH is higher than the isoelectric point (IEP) of the metal; which tends to be above pH 9. Thus at pH < 9 the surface is positively charged. Microbes tend to be negatively charged so it is expected that a decrease in pH would result in an increase in adhesion.

Vadillo-Rodriguez et al., (2005) used AFM to determine the force of adhesion of bacteria with and without single layer protein (SLP) to hydrophobic and hydrophilic AFM tips (in concentrations of 10 and 100 mM). At low ionic strength the lowest and highest adhesion force was recorded for the hydrophilic tip with and without the SLP respectively but this was reversed when tested at higher ionic strength. Bowen et al., (2001) used AFM to study yeast cell detachment from mica surfaces with specific properties: (i) hydrophilic, (ii) hydrophobic and (iii) bovine serum albumin (BSA) coated at pH 5 (0.01 M BSA). The greatest adhesion was measured at the hydrophobic surface (46.6 ± 20.8 nN). Hydrophilic and BSA-coated mica were found to exhibit similar adhesive strengths at 9.7- 10.2 nN (± 5.1 and 9 nN respectively).

Fang et al., (2000) used AFM to quantify the adhesion between a Si_3N_4 cantilever tip and a biofilm of sulphate reducing bacteria on a mica surface. When the tip was positioned over different points on the same bacterium, the adhesion force measured at the periphery was greater than on the cell surface. This was attributed to the accumulation of EPS (extracellular polymeric substance) at the cell-mica interface. Bowen et al., (2001) also found that yeast-mica contact time was important because after 5 minutes the adhesion force increased by 20 nN.

1.2.2 NON-MICROBIAL ADHESION

A number of authors have studied non-microbial adhesion behaviour using AFM. Bruinsma et al., (2001) used AFM to determine contact lens roughness and to visualise the adhesion of human tears to hydrophilic and hydrophobic contact lenses. Adhesion of the tear solution to both lenses revealed a similar roughness of 13 – 16 nm.

Handojo et al., (2009) used AFM to determine the adhesive properties and film thickness of chocolate milk, whole milk, 2% fat milk and skimmed milk residues on glass following washing. All materials had adhesion values of 94 - 97 mN m^{-1}. Skimmed and 2% fat milk exhibited higher moisture contents than chocolate and whole milk, which corresponded to higher values for the work of adhesion (> 96 mN m^{-1}). The whole and chocolate milk presented larger residue film thicknesses, approximately 225 ± 30 nm and approximately 120 ± 90 nm, respectively.

Parabhu et al., (2006) used AFM to determine the IEP of a chromium oxide surface with and without sodium silicate treatment. The authors showed there was no significant difference in surface IEP after sodium silicate treatment, it was merely lowered. It was suggested that phosphate ions bound to the surface reducing binding sites for milk components. The authors also demonstrated that a much lower

change in pressure drop was achieved by treating the surface (3 – 4.2 kPa), indicating much less fouling than an average run (pressure drop of 14.5 kPa), confirmed by visual inspection.

Wu et al., (2008) used AFM to measure the effect of nanobubbles on fouling and cleaning of a graphite cathode. Nanobubbles generated electrochemically and situated on the cathode could significantly reduce adsorption of BSA (10-20 μg mL^{-1}). Cleaning of BSA from the cathode and a SS surface with nanobubbles was compared to water and electrolyte washing. In the case of the cathode, minimal BSA was removed by washing but nanobubbles removed 82% of the initial fouling monolayer. For the steel surface, minimal protein was removed by multiple washes (~ 15%), whilst for a similar number of nanobubble treatments 60 % of protein was removed (1 treatment was 3 minutes of washing or bubbles). The application of nanobubbles may be useful for the regeneration of fouled filters and in controlling microbial adsorption.
Previous work from Akhtar et al., (2010) compared adhesion of a range of food and personal care foulants to different surfaces: SS, glass, and trichloro(3,3,3-trifluoropropyl)silane – a model for fluoropolymer surfaces such as poly(tetrafluoroethylene). Particle tips of the different materials were attached to the AFM cantilever to study the detachment from toothpaste and confectionary components: Turkish delight, caramel and sweetened condensed milk (SCM). Significantly different detachment forces were measured at room temperature for the same deposit from different surface types.

One important property is the adhesion of food products at different processing temperatures. The aim of this paper is to use AFM to study adhesion between deposits and different surfaces at process temperatures. SS and hydrophobic poly(tetrafluoroethylene)-analogue surfaces have been studied. Research describing the relationship between temperature and material adhesion to food contact surfaces by AFM is limited. Capella and Stark (2006) tested the work of adhesion from 33 to 51°C of an amorphous polymer and polystyrene to an AFM cantilever tip. They suggested as the temperature was increased, the work of adhesion increased. Lam and Newton (1992) investigated the adhesion of calcium carbonate to SS at -15, 0, 10 and 20°C. The authors found a linear relationship between temperature and adhesion force. This paper presents data on the adhesion behaviour of confectionary (sugar-based) products: caramel and SCM at different temperatures using AFM. The adhesion behaviour is compared to whey protein, which contains the protein β-lg which forms most of milk pasteuriser deposit.

2. MATERIAL AND METHODS

2.1 AFM EQUIPMENT AND OPERATION

Experiments were carried out using a NanoWizard II AFM adapted to include a Heating/Cooling Stage (JPK Instruments, UK). The lateral scan range was 100 µm x 100 µm and the vertical range was 15 µm, enabling acquisition of force data for sticky deposits. JPK data processing software was used for all analyses. Topographic imaging of a sample can be attempted using contact mode or intermittent contact mode**.** For data presented here, contact mode was used, in which mode the cantilever tip is in direct contact with the surface, under a compressive load of the order 10 nN, and as the tip moves across the surface the change in cantilever deflection is monitored via the change in the position of the laser beam on the photodiode. A feedback control system is used to maintain the setpoint compressive load between the cantilever and the surface. Adhesion force measurements were performed using modified tipless Si cantilevers of nominal length 225 µm, nominal force constant 48 N m^{-1} and nominal resonance frequency 190 kHz (Windsor Scientific, UK).

2.2 AFM TIP MODIFICATION

Commercially available AFM tips are pre-made with different attached materials such as silica of different sizes and are very expensive. The adhesive interactions between model food deposits and SS and fluoro-coated glass are of interest here. As it was easier to functionalise the tips with the surface materials than with the deposits, experiments were conducted using the following materials as AFM colloid probes:

- SS 316L microparticles of 30 µm diameter (Reade, USA). These are hereafter referred to using the acronym SS.
- Glass microparticles of 30 µm diameter (Polysciences, UK) coated with a 200 nm thick film of vapour-deposited trichloro(3,3,3-trifluoropropyl)silane (Aldrich, UK); this is thus a highly hydrophobic surface. These are hereafter referred to using the acronym FCG, i.e. fluoro-coated glass.

5 mL of trichloro(3,3,3-trifluoropropyl)silane (in a Petri dish) and glass microparticles were put in glass dessicator and placed under vacuum for 24 h. The FCG microparticle coating thickness was measured using AFM.

To attach the microparticle of interest to a tip, a 0.2 mL droplet of epoxy adhesive (Araldite, UK) was placed on a glass slide. Using the video microscope system incorporated into the AFM a tipless Si cantilever was brought into contact with the glue. By comparing the size of the droplet on the slide before and after contact with the AFM tip, one can estimate the amount of epoxy deposited onto the tip by trial and error. The amount of deposited epoxy should not be more than a few cubic microns. The glue was allowed to semi-cure on the cantilever free end before the microparticle of interest, SS or FCG, was attached at the free end and left for 5 minutes to adhere (for further details see Akhtar, 2010).

2.3 RAW MATERIALS

All products selected for investigation become type 3 foulants when heated (see Fryer and Asteriadou, 2009 for details), i.e. they require chemical for removal. Food material details and preparation procedures are given below. Products were used in the condition described below, without any further dilution or preparation. For further details see Akhtar (2010).

(i) **WPC**: WP35 powder (Carberry, Ireland) was used to make a whey protein solution with a final β-lg concentration of 0.3 wt% (typical of milk). WP35 powder had approximately 15 wt% β-lg. Water and whey protein powder were mixed using an electronic mixer to ensure the solution was homogeneous; which took approximately 10 minutes. The solution was left for a further 20 minutes at room temperature to de-aerate before application to surfaces. Approximately 98% of the solution was water.

(ii) **SCM** (Cadbury, UK): SCM is derived from milk, heated to 85 - 90°C for several seconds to remove water. Sugar is then added to sweeten the product and increase product shelf life. SCM is 50 % sugar, 15% skim milk solids, 5 % fat.

(iii) **Caramel:** (Cadbury, UK). Caramel is derived from the polymerisation of sugars heated slowly to high temperature. The action of heating and various additions removes water and increases product viscosity. Caramel is 75 % sugar, 5 % WPC, 11 % fat.

2.4 Deposit Immobilisation

The deposits mentioned in §2.3 were immobilised onto glass slides (Agar Scientific, UK) using a small syringe needle (Fisher Scientific, UK). All sample handling was carried out using Dumostar tweezers (Agar Scientific, UK) to minimise the risk of sample contamination. A deposit film 50-60 µm thick was determined using the AFM optical system. The cantilever was engaged towards the deposit and force measurements taken. The tip was cleaned after each experiment by immersion in a large volume of HPLC water (Fisher Scientific, UK). A minimum of five measurements were performed per probe/deposit combination. JPK data processing software (JPK, Berlin) was used for both real-time analysis and post-capture image processing.

2.5 Experimental Conditions

The variable parameters used in experiments were:

(i) *Different particle tips:* SS and FCG; a typical food contact surface and a typical 'low adhesion' contact surface respectively.

(ii) *Different temperatures:* all materials were studied at 30ºC, 50ºC, 70ºC, and 90ºC using a heating stage incorporated into the AFM. The deposits were first heated for 5 minutes during which the temperature was monitored and maintained before adhesion forces were measured during probe retraction.

(iii) *Different Contact Times:* Retraction data were recorded for different probe/deposit contact times ranging from 0 s, where the probe touches the deposit and fixed end retraction commences within 0.2 s, and extended contact durations of 0.5, 1, 5, 10, 20 and 60 s. The probe and deposit contact could be seen using the AFM camera and microscope. No data could be obtained for caramel at contact times > 5 s because the deposit engulfed the microparticle, deflecting the cantilever sufficiently that retract would not occur within the range of the deflection detection system.

(iv) *Different tip retraction velocity*: The velocity at which the fixed end is retracted away from the deposit was varied between at 0.25, 0.75, 1, 3 and 5 µm s^{-1}. These velocities were chosen to be within the size (40-50 µm) of sample used and the maximum vertical travel limits of the AFM.

2.6 Minimizing Experimental Variation

Factors found to contribute to experimental variation include:

(i) *Moisture loss from materials*: variation of the material composition was minimised by doing experiments one at time: deposits were used quickly to minimise any moisture change. Also the same batch of raw material (WPC, SCM or caramel) was used to complete the data set.

(ii) *Cantilever and tip integrity*: Switching the cantilevers and cleaning the tips during experimental work could damage the components, contaminate the tips and create errors. To avoid this each deposit was studied using its own cantilever which was cleaned regularly of deposit. The cantilever shape was analysed regularly under the microscope, and the tilt and the spring constants were measured regularly to ensure data obtained was accurate.

(iii) *Inaccuracy of equipment:* Image resolution and force measurements can fluctuate with changing noise level, to minimise against this the AFM was mounted on a vibration isolation table and only one operator was in the room performing measurements.

Each experiment was conducted at least three times to assess the measurement consistency. The average value is plotted in each case and the data shows a global variation of the mean is plotted as the error.

2.7 RHEOLOGY

An AR1000 rheometer (TA Instruments, Coventry, UK) and SS cone geometry (40 mm, 52 μm gap) was used to determine the viscosity of SCM and caramel supplied by Cadbury (Birmingham, UK). A similar amount of each sample was added to the heating stage for each experiment and the moisture trap positioned to prevent excess water evaporation during experimentation. Each sample was left for up to 5 minutes at the test temperature to equilibrate before testing. At least two replicates of each measurement were made to assess reproducibility. Data for whey protein was taken from Tang et al., (1993).

3. RESULTS

The wettability of the two microparticle types and the viscosity of each deposit is presented in the first section. The adhesion data collected is presented in three sections, *the effect of the retraction rate:* in the range 0.25 – 5 µm s^{-1}. *The effect of surface and temperature:* SS and FCG; 30, 50, 70 and 90°C; *the effect of contact time*: in the range 0 – 60 s.

3.1 CHARACTERISATION OF SURFACE AND DEPOSIT

Akhtar (2010) characterised the contact angle using a Goniometer (Krüss, Bristol) to assess the surface energies of SS and FCG with a drop of water. Contact angles were found to be 92 ± 2° and 106 ± 4° for SS and FCG respectively, indicating a partial wetting and relatively non-wetting surface. The surface free energy was found to be 0.07 ± 0.001 mJ m^{-2} for SS and 0.05 ± 0.001 mJ m^{-2} for FCG.

The viscosity of SCM and caramel at a range of temperatures is presented in Figure 1. Each deposit was allowed to equilibrate for 5 minutes before testing. As the temperature was increased, viscosity decreased. The viscosity of WPC (15 % solids) is also presented from Tang et al., (1993). The WPC was held for 2 minutes at each temperature before testing. Viscosity data in the range 5-65°C is presented for WPC. After this point, 70-74°C the viscosity increases indicating WPC aggregation and denaturation.

Figure 2 is a schematic detailing the key features of a typical AFM force measurement during probe retraction. The fixed end of the cantilever is driven away from the deposit at a fixed velocity; the response of the free end of the cantilever is recorded and plotted versus the fixed end displacement. The probe moves quickly from being in a compressive regime, following the approach portion of the measurement, into a tensile regime, indicative of the adhesion between the probe and the deposit. The magnitude of the adhesion reported hereon corresponds to the peak force recorded, F_{max}.

3.2 THE EFFECT OF SURFACE AND TEMPERATURE ON ADHESION

Figures 3-5 summarise the maximum measured adhesion forces measured for WPC, SCM and caramel respectively in contact with (a) a SS microparticle and (b) a FCG microparticle. The data is plotted to illustrate the adhesion force at each temperature: 30, 50, 70 and 90°C, and for increasing contact times ranging from 0 to 60 s; 0 s being where the tip touches the sample, and then is retracted instantly, which corresponds to a finite contact time < 0.2 s.

3.2.1 WPC

Figure 3 illustrates that the adhesion force of WPC at 90°C (approximately 0.60 N m^{-1}) is significantly higher than at 70, 50 and 30°C (approximately 0.02 N m^{-1}) and is also significantly higher than the adhesion force of the microparticles to SCM and caramel. The adhesion force of WPC to both microparticle types is significantly high at 90°C with low variation, at approximately 0.6 ± 0.004 N m^{-1}. At 90°C the adhesion force of both microparticles to WPC is similar. It may be the case that van der Waals forces are the dominant contribution towards the adhesion of WPC to SS and FCG. Hence, it might be reasonable to expect that the adhesion forces for these two probe/deposit combinations would be similar, as the only contribution towards adhesion would arise from dispersion forces.

3.2.2 SCM

Figure 4 illustrates that the adhesion force of SCM to the SS and FCG microparticle is similar at all temperatures, in the range 0.27-0.35 N m^{-1} except at 30°C for FCG. The adhesion of SCM to the FCG microparticle was significantly lower at 30°C. This finding illustrates the importance of studying the adhesion of food stuffs to 'non-stick' surfaces at a range of typical processing temperatures. The

adhesion of SCM to TCTFS is greater at higher temperatures. The error is reasonably consistent except at the shortest contact time where it is very large so no conclusions can be drawn here.

3.2.3 Caramel

Figure 5 illustrates that the adhesion force of caramel to SS and FCG is quite different. At 0 s contact time, adhesion of caramel to (a) SS appears to decrease with increasing temperature whereas the adhesion to (b) FCG appears to decrease with increasing temperature. The adhesion force exhibited by FCG/caramel was also greater than that exhibited by SS/caramel at 0 s contact time. An increase in contact time changes this behaviour, discussed in the next section. The largest adhesion force was measured at 30°C for both surfaces; 0.41 N m^{-1} for SS and 0.3 N m^{-1} for FCG. This is different to WPC and SCM where the highest adhesion forces were measured at 90°C, 0.6 and 0.3 N m^{-1} respectively. The error is consistently low for data measured using the FCG microparticle. The error is larger and more inconsistent for data measured using the SS microparticle.

3.3 The Effect of Contact time between probe and deposit adhesion

3.3.1 WPC

Figure 3 illustrates the effect of increasing contact time between the probe and WPC deposit to (a) SS and (b) FCG. The error is reasonably consistent in almost all cases. It is clear that high temperature rather than contact time governs the adhesion force of WPC to SS and FCG. It does appear however that at 90°C as the contact time of FCG and WPC is increased the adhesion force increases slightly from 0.56 ± 0.004 N m^{-1} to 0.62 ± 0.001 N m^{-1} over the contact time range; this increase may be due to small increases in the deposit/probe contact area as the probe is held in contact with the deposit.

WPC adhesion to the SS microparticle also increases significantly with contact time for measurements performed at 70°C. This sudden increase occurs between contact times of 10 s and 20 s with a large increase in adhesion force from approximately 0.02 N m^{-1} at 0-10 s to 0.30-060 N m^{-1} at 20-60 s. Interestingly, at the longer contact times of 20 s and 60 s there is a significant decrease in the adhesion force at 90°C, from 0.6 ± 0.001 N m^{-1} to 0.3 ± 0.003 N m^{-1}. These findings indicate that the contact time between a deposit and a surface at high temperature is important in governing the adhesive strength. As the contact time is increased at 70°C, WPC likely denatures and adheres more strongly to the surface. Simmons et al., (2007) revealed that larger aggregates of WPC were formed at 90°C compared to 75°C, and in a shorter time, in 5 minutes rather than 20 minutes. This demonstrates the propensity of WPC to denature increasingly rapidly at temperatures above 70°C. The impact of this finding for process fouling is that holding WPC at temperatures greater than 70°C for extended periods of time may result in strongly adhesive deposits which will be difficult to remove.

3.3.2 SCM

Figure 4 illustrates there is no obvious trend in the data for SS contact times of 10 s and lower. At 20 s and 60 s however, an increase in temperature decreases the adhesion force. Also at 30°C an increase in contact time from 0.5 s to 60 s increases the force of adhesion from 0.27 to 0.35 N m^{-1}. The largest adhesion force 0.35 ± 0.009 N m^{-1} was measured at the lowest temperature and the longest contact time, 30°C and 60 s.

For SCM adhesion to FCG the relationship is quite different to that of SS and SCM. The adhesion force measured at 70 and 90°C is consistent for all contact times, approximately 0.3 N m^{-1}. At 30°C and contact times of up to 10 s the adhesion force is consistently low, 0.01 N m^{-1}. However an increase in

contact time to 10, 20 and 60 s reveals an increase in the adhesion force from 0.24 to 0.3 N m^{-1}. This adhesive force is of a similar value to that measured at 70 and 90°C.

3.3.3 Caramel

Figure 5 illustrates there is no obvious trend in the adhesion data for increasing contact time between the SS microparticle and caramel. Similarly to SCM, the largest adhesion force 0.41 ± 0.0003 N m^{-1} was recorded at the lowest temperature with the longest contact time, 30°C and 10 s. No obvious trend was seen in the data as the contact time was increased, similarly to SCM data. This may be because a contact time of longer than 10 s is needed to see a relationship. Alternatively, there is no relationship. Adhesion data for caramel was measured at shorter contact times than SCM, 10 s or less, due to the phenomenon observed at longer contact times whereby microparticles became engulfed by the deposit.

The adhesion data for FCG is also quite different to that of the SS microparticle. At 0 s contact time the largest adhesion force is measured at 30°C (0.3 ± 0.002 N m^{-1}) and this decreases as the temperature is increased to 90°C (0.2 ± 0.002 N m^{-1}). Interestingly, an increase in contact time reduces all adhesion forces to approximately 0.02 N m^{-1}. However data was only collected for contact times of a maximum of 5 s due to the phenomenon observed at longer contact times whereby microparticles became engulfed by the deposit.

3.4 The Effect of Probe retraction Rate

The cantilever tip was held in contact with each deposit for 5 s before retraction. The retract speeds investigated were 0.25, 0.75, 1.0, 1.5, 3 and 5 µm s^{-1}. No significant effect of cantilever retraction rate on deposit adhesion data was seen. This may be due to the short contact time between the deposit and microparticle at each temperature.

4. DISCUSSION

It was expected that the adhesion force between microparticle and deposit would increase with temperature, as fouling in plate heat exchangers increases at ca. 75°C as a result of whey protein (β-lg) denaturation and aggregation. The results suggest that this is true for WPC adhesion to both SS and FCG, a perceived 'no-stick' coating. The adhesive force of WPC to SS and FCG is significantly high at high temperature regardless of the contact time.

Deposits have been demonstrated in many cases to form at high processing temperatures. For caramel and SCM, adhesion to the SS microparticle was greatest at the lowest temperature and longest contact time. This is different to the adhesion behaviour of WPC. This may be due to the material compositions. WPC is predominantly protein whereas confectionary deposits are predominantly sugar and fat. The adhesion force of these materials may decrease due to the decreasing material viscosity, provided that the temperature increase is insufficient to cause caramelisation and polymerisation of the sugars and fats. This process typically occurs at temperatures much greater than 90°C. The caramelisation and polymerisation of the sugars and fats is an analogous process to the denaturation of the WPC. Hence, it might be expected that if temperatures sufficiently high to cause caramelisation and polymerisation of the sugars and fats were investigated, the confectionary deposits would also exhibit strong adhesion to the probe surface.

Interestingly, the adhesion of caramel to FCG decreases with increasing temperature and increasing contact time, whereas SCM adhesion to FCG is consistently high at 70 and 90°C at all contact times. Perhaps because caramel data was only collected for contact times of up to 5 s in this case, if it was possible to observe longer contact times the adhesion force of caramel may have increased with increasing temperature and time. It is possible that this could be achieved using a macroscopic approach.

It was possible to relate data from the AFM to measurements taken using micromanipulation probes (Liu et al, 2002, 2005, 2006, 2007) on millimetre-scale deposits, suggesting that data from the nanoscale could be scaled up to the meso-scale. The importance of the scale of measurement was also demonstrated by Wyart et al., (2008) who characterised the roughness of unused ceramic membranes by three different microscopic techniques: SEM, AFM and WLI (white light interferometry). Deposit adhesion at the nanoscale and at the microscale may be different. At the microscale material properties such as viscosity or viscoelasticity could play a part in determining overall adhesion force. Such properties are inherent to the deposit and relatively surface-independent. However from the results presented here, the viscosity and the adhesion forces measured at increased temperatures and contact times seem to agree. As such, it may be possible to say that a 'non-stick' pipe may reduce adhesion during pumping of confectionary product at low temperatures. However use of a 'non-stick' pipe in a heated process line may result in a similar level of fouling to that of a SS pipe. The development of candidate antifouling surfaces (such as those proposed by Rosmaninho et al., 2005, 2003) will require understanding of how adhesion happens at processing temperatures. More work is needed to determine what effects reaction processes have on adhesion at these temperatures.

5. CONCLUSION

AFM force measurement experiments have been conducted over a range of deposits, temperatures, surface types, contact times and retraction rates. The following conclusions can be drawn:

- WPC adhesion to both surface probes is significantly large for all contact times at 90°C. An increase in contact time also increases the significance of WPC adhesion SS at 70°C.
- For confectionary deposits adhesion to SS was similar. Adhesion measured at 30°C was significantly larger than at other temperatures. However the difference between adhesion forces measured at different temperatures were not as vastly different as in the WPC case. Adhesion of confectionary deposits to FCG at 30°C revealed a decrease in adhesion compared to SS, however at higher temperatures and longer contact times the adhesion force remained as high as adhesion to SS.
- The effect of retraction rate does not affect adhesion measurement in this case.

The data presented here suggests that measuring adhesion at real process temperatures is valuable and can provide data that is significantly different from room temperature measurements. As such any effective models for fouling or cleaning must account for adhesion forces at higher temperatures.

References

Akhtar, N., 2010, The fundamental interactions between deposits and surfaces at nanoscale using atomic force microscopy, School of Chemical Engineering, PhD Thesis, University of Birmingham.

Akhtar, N., Bowen, J., Asteriadou, K., Zhang, Z., Fryer, P.J., 2010, Matching the nano- to the meso-scale: Measuring deposit–surface interactions with atomic force microscopy and micromanipulation, Food and Bioproducts Processing, 88: 341-348.

Binnig, G., Quate, C.F.. Gerber, C. 1986, Atomic force microscope, Physical Review Letters, 56: 930–933.

Bowen, W.R., Lovitt, W.R., Wright, C.J., 2000, Direct quantification of *Aspergillus niger s*pore adhesion in liquid using an atomic force microscope, Journal of Colloid and Interface Science, 228: 428–433.

Bowen, W.R., Lovitt, W.R., Wright, C.J., 2001, Atomic force microscopy study of the adhesion of *Saccharomyces cerevisiae*, Journal of Colloid and Interface Science, 237: 54–61.

Bruinsma, A.M., Van der Mei, H.C., Busscher, H.J., 2001, Bacterial adhesion to surface hydrophilic and hydrophobic contact lenses, Biomaterials, 22: 3217 – 3224.

Capella, B., Stark, A., 2006, Adhesion of amorphous polymers as a function of temperature probes with AFM force-distance curves, Journal of Colloid and Interface Science, 296: 507-514.

Changani, S.D., Belmar-Beiny, M.T., Fryer, P.J., 1997, Engineering and chemical factors associated with fouling and cleaning in milk processing, Experimental Thermal and Fluid Science, 19: 392-406.

Christian, G.K, Fryer, P.J., 2006, The effect of pulsing cleaning chemicals on the cleaning of whey protein deposits, Trans IChemE, Part C, Food and Bioproducts Processing, 84: 320–328.

Fang, H.H.P., Chan, K.W., Xu, L.C., 2000, Quantification of bacterial adhesion forces using atomic force microscopy (AFM), Journal of Microbiological Methods, 40: 89-97.

Fryer, P.J., Asteriadou, K., 2009. A Prototype cleaning map: a classification of industrial cleaning processes. Trends in Food Science & Technology, 20, 225–262.

Fryer, P.J., Christian, G.K., Liu, W., 2006, How hygiene happens: physics and chemistry of cleaning, International Journal of Dairy Technology, 59: 76-84.

Handojo, A., Zhai, Y., Frankel, G., Pascall, M.A., 2009, Measurement of adhesion strengths between various milk products on glass surfaces using contact angle measurement and atomic force microscopy, Journal of Food Engineering, 92: 305-311.

Lam, K.K., Newton, J.M., 1992, Effect of temperature on solid adhesion to a substrate surface, Powder Technology, 73: 267-274.

Liu, S., Wang, Y., 2011, A review of the application of atomic force microscopy (AFM) in food science and technology, In: *Advances in Food and Nutrition Research.* Elsevier, USA.

Liu, W., Aziz, N.A., Zhang, Z., Fryer, P.J., 2007, Quantification of the cleaning of egg albumin deposits using micromanipulation and direct observation techniques, Journal of Food Engineering, 78: 217-224.

Liu, W., Christian, G.K., Zhang, Z., Fryer, P.J., 2002, Development and use of a micromanipulation technique for measuring the force required to disrupt and remove fouling deposits, Food and Bioproducts Processing, 80: 286-291.

Liu, W., Christian, G.K., Zhang, Z., Fryer, P.J., 2006, Direct measurement of the force required to disrupt and remove fouling deposits of whey protein concentrate. International Dairy Journal, 16: 164-172.

Liu, W., Fryer, P.J., Zhang, Z., Zhao, Q., Liu, Y., 2006, Identification of cohesive and adhesive effects in the cleaning of food fouling deposits, Innovative Food Science & Emerging Technologies, 7: 263-269.

Morris, V.J., 2004 Probing molecular interactions in foods, Trends in Food Science & Technology, 15: 291–297.

Parabhu, A., Hendy, S., Danne, M., 2006, Reducing milk protein adhesion rates a transient surface treatment of stainless steel, Food and Bioproducts Processing, Trans IChemE Part C, 84: 274-278.

Rosmaninho, R. Rizzo, G. Müller-Steinhagen, H. Melo, F., 2005, Anti fouling stainless steel based surface for milk heating processes, *Heat Exchanger Fouling and Cleaning*, German Aerospace Centre, Stuttgart, Germany, the University of British Columbia, Canada Eds, ECI Symposium Series, Volume RP2.

Rosmaninho, R. Rizzo, G. Müller-Steinhagen, H. and Melo, L. F., 2003, The influence of bulk properties and surface characteristics on the deposition process of calcium phosphate on stainless steel. In: *Heat Exchanger Fouling and Cleaning Fundamentals and Applications,* Santa Fe, New Mexico, USA.

Sheng, X., Ting, Y.P., Pehkonen, S.O., 2008, The influence of ionic strength, nutrients and pH on bacterial adhesion to metals, Journal of Colloid and Interface Science, 321: 256-264.

Simmons, M.J.H., Jayaraman, P., Fryer, P.J., 2007, The effect of temperature and shear rate upon the aggregation of whey protein and its implications for milk fouling, Journal of Food Engineering, 79: 517-528.

Tamine, A.Y., 2008, Cleaning-in-Place: Dairy, Food and Beverage Operations, Blackwell, Oxford.

Tang, Q., Munro, P.A., McCarthy, O.J., 1993, Rheology of whey protein concentrate solutions as a function of concentration, temperature, pH and salt concentration, Journal of Dairy Research, 60: 349.

Vadillo-Rodríguez, V., Busscher, H.J., van der Mei, H.C., de Vries, J., Norde, W., 2005, Role of lactobacillus cell surface hydrophobicity as probed by AFM in adhesion to surfaces at low and high ionic strength, Colloids and Surfaces B: Biointerfaces, 41: 33 – 41.

Verran, J., Rowe, D.L., Cole, D., Boyd, R.D., 2000, The use of the atomic force microscope to visualise and measure wear of food contact surfaces, International Biodeterioration & Biodegradation, 46: 99-105.

Whitehead, K.A., Rogers, D., Colligon, J., Wright, C., Verran, J., 2006, Use of the atomic force microscope to determine the effect of substratum surface topography on the ease of bacterial removal, Colloids and Surfaces B: Biointerfaces, 51: 44–53.

Wu, Z., Hongbing, C., Yaming, D., Huiling, M., Sun, J., Chen, S., Craig, V.S.J., Hu, J., 2008, Cleaning using nanobubbles: defouling by electrochemical generation of bubbles, Journal of Colloid and Interface Science, 328, 10-14.

Wyart, Y., Georges, G., Deumie, C., Amra, C., Moulin, P., 2008, Membrane characterization by microscopic methods: multiscale structure, Journal of Membrane Science, 315: 82-92.

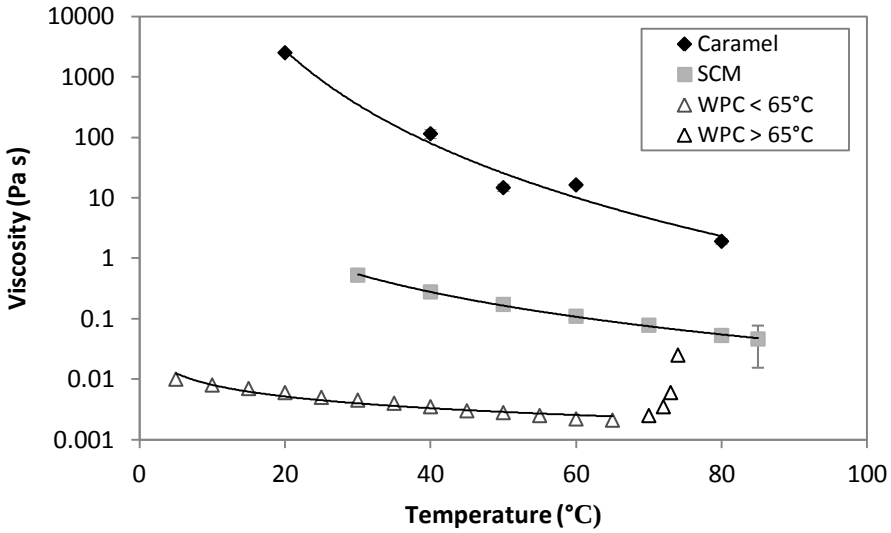

Figure 1: Plot of Viscosity vs. Temperature for WPC (15% solids; 291 s^{-1} from Tang et al., 1993), SCM (Cadbury, Birmingham) and Caramel (Cadbury, Birmingham).

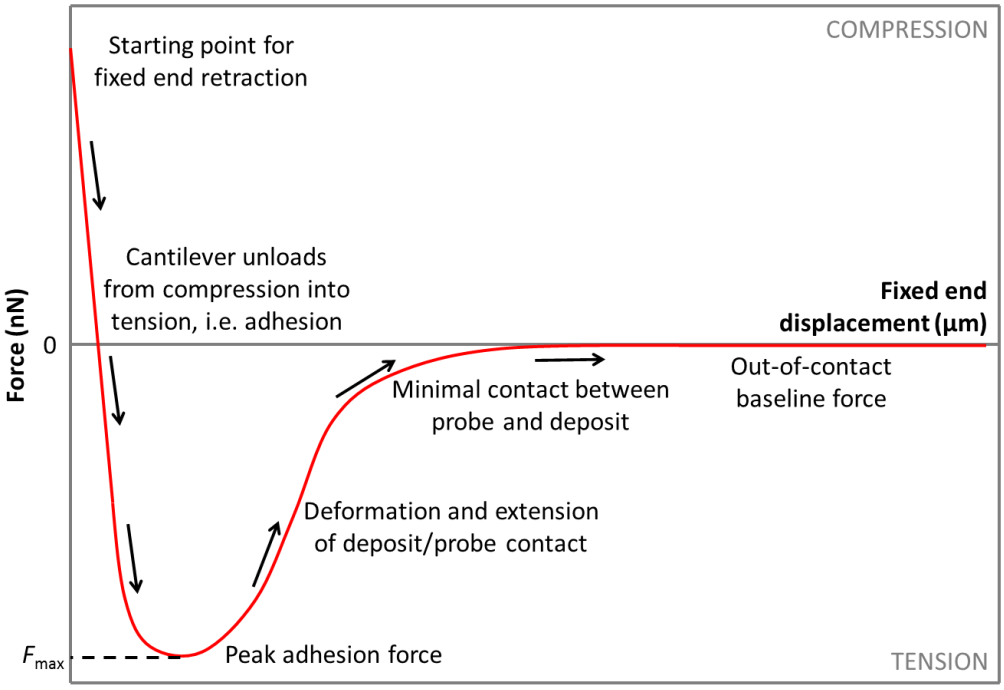

Figure 2: Schematic detailing key features of a typical AFM force measurement during probe retraction.

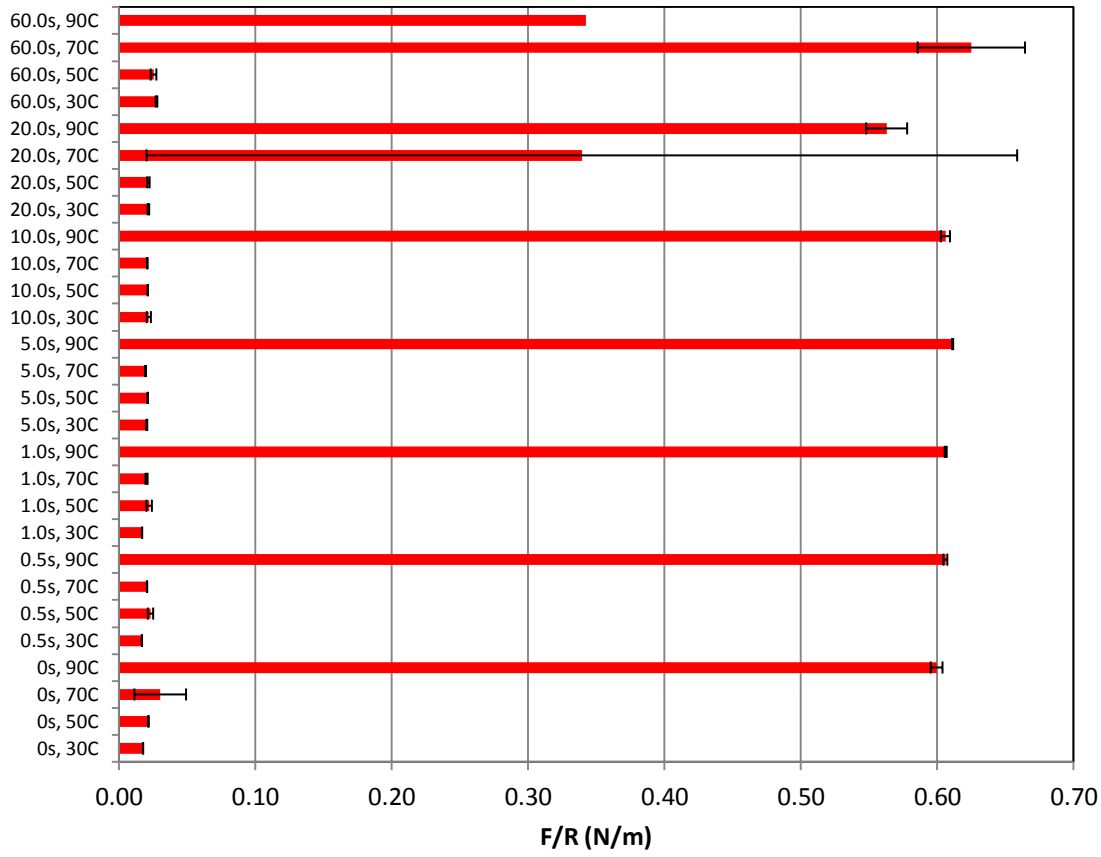

(a)

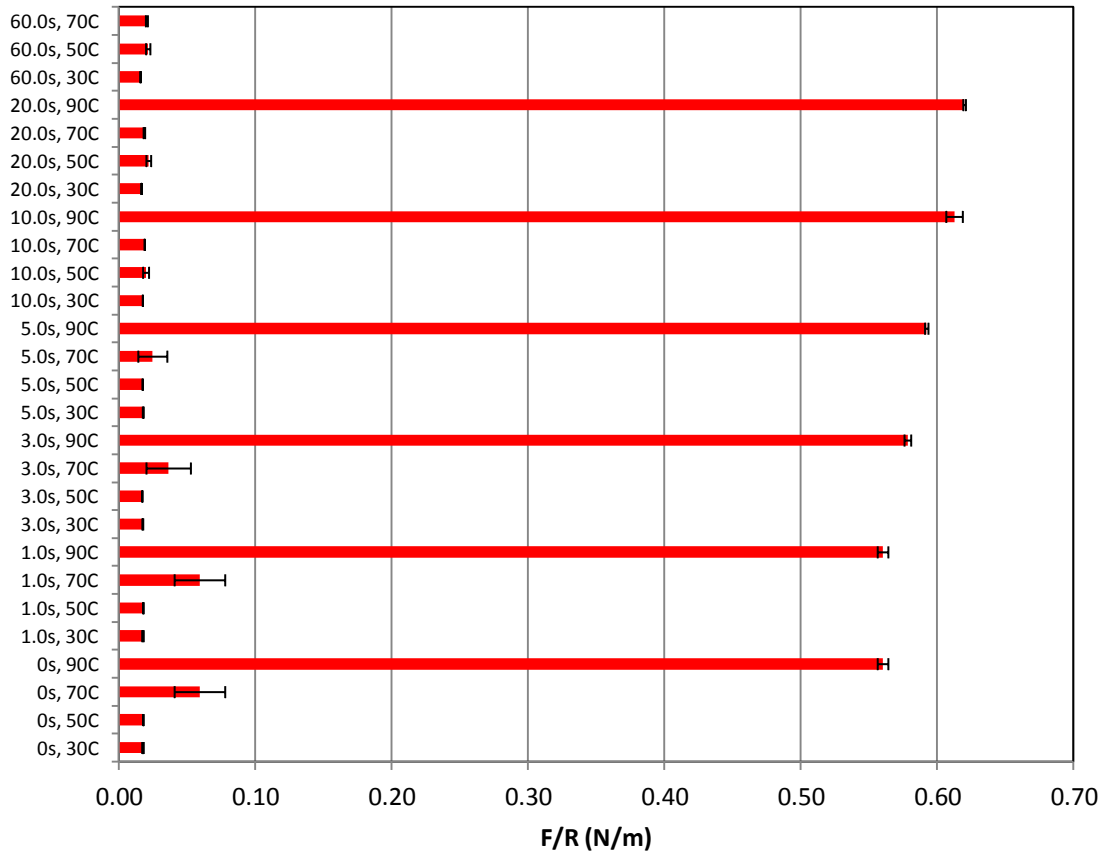

(b)

Figure 3: Force measurements of (a) SS microparticle and (b) FCG immersed in WPC and then retracted off the deposit. The approach speed for all experiments was 3 µm s^{-1}, then a stationary contact time on the deposit (indicated for each experiment), and a final retraction rate of 0.25 µm s^{-1}. The data shows a global variation of the mean of at least three experiments.

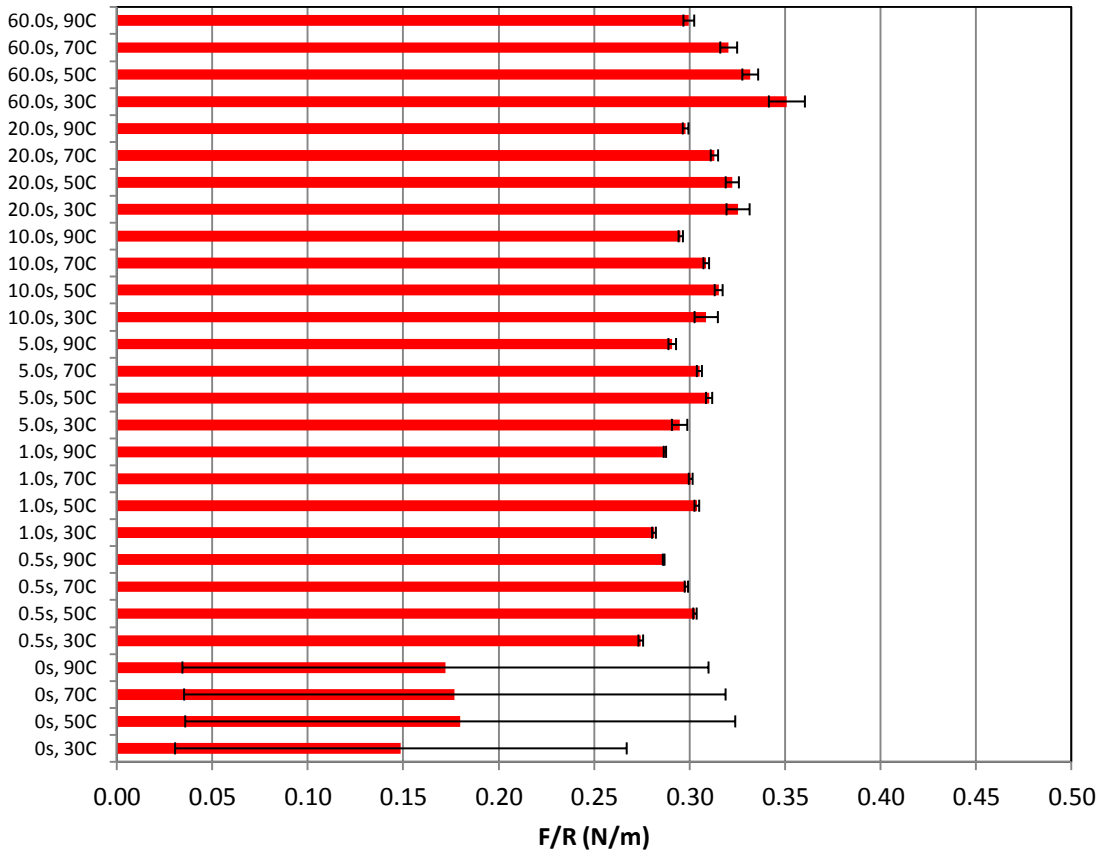

(a)

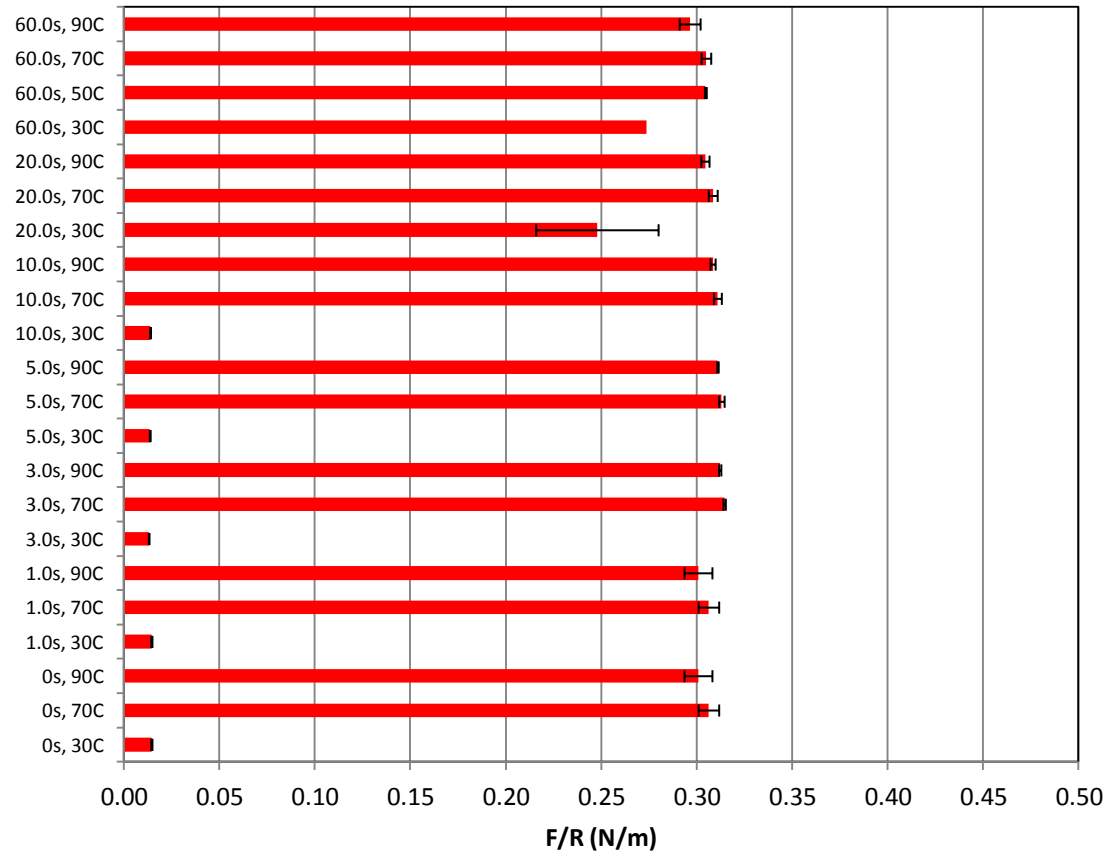

(b)

Figure 4: Force measurements of (a) SS microparticle and (b) FCG immersed in SCM and then retracted off the deposit. The approach speed for all experiments was 3 µm s^{-1}, then a stationary contact time on the deposit (indicated for each experiment), and a final retraction rate of 0.25 µm s^{-1}. The data shows a global variation of the mean of at least three experiments.

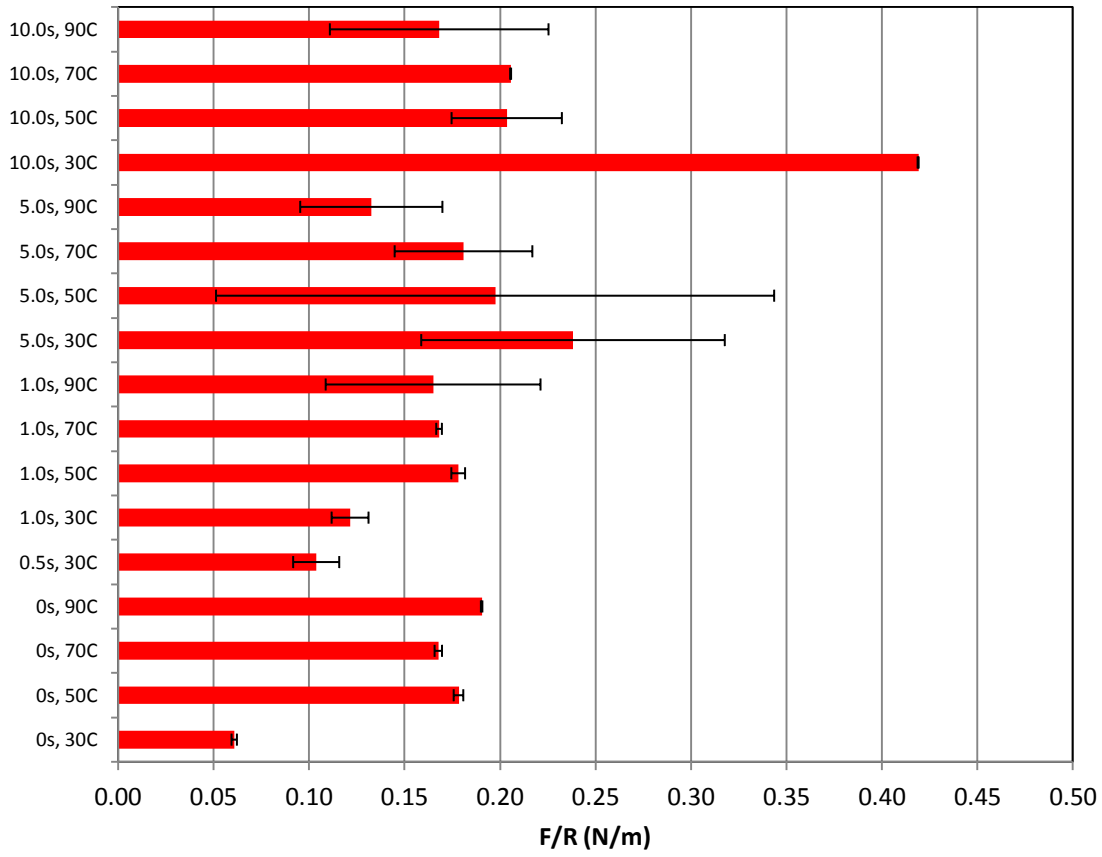

(a)

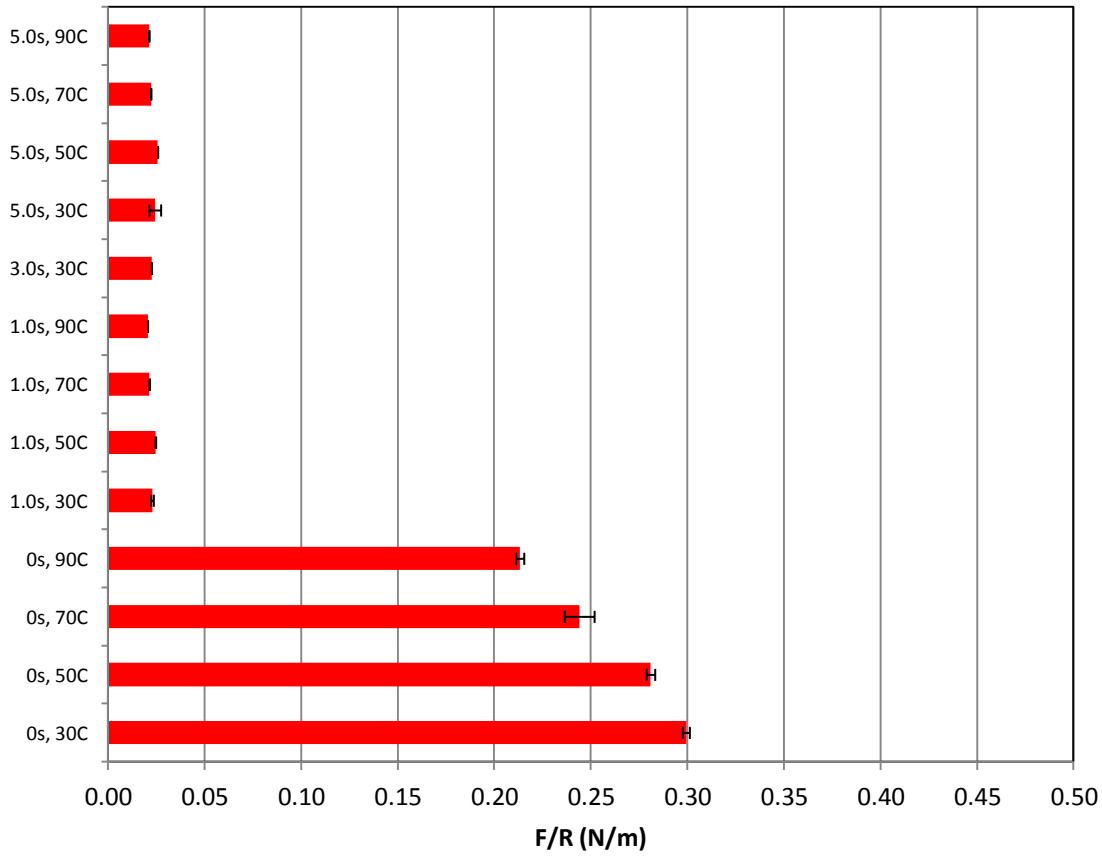

(b)

Figure 5: Force measurements of (a) SS microparticle and (b) FCG immersed in caramel and then retracted off the deposit. The approach speed for all experiments was 3 µm s^{-1}, then a stationary contact time on the deposit (indicated for each experiment), and a final retraction rate of 0.25 µm s^{-1}. The data shows a global variation of the mean of at least three experiments.